Supplementary document: Kinematics of Drawing Machines

Robin Roussel[1,2] Marie-Paule Cani[2] Jean-Claude Léon[2] Niloy J. Mitra[1]

[1]University College London [2]Grenoble Alpes University, INRIA

1 Introduction

This supplement describes the parameterization and kinematic behavior of the drawing machines supported by our system. For each machine, we present the following elements.

- **Design parameters.** These parameters describe the layout and physical dimensions of the components of a machine. They can be continuous or discrete.
- **Constraints on design parameters.** These constraints translate high-level feasibility requirements and symmetry reductions (see typology below) into a set of (in)equalities.
- **Kinematic equations.** The pattern drawn by a machine is expressed as a function of time and design parameters.

1.1 Time interval

Although the kinematic equations were obtained using a geometric approach, their time-periodicity can be determined by applying modular arithmetic on a subset of the design parameters. Let us first consider a pair of meshing gears, G_1 and G_2, which both influence the drawing pen. We note their (equivalent) radii r_1 and r_2, which we assume to be integers. The law of gearing gives:

$$\frac{r_1}{r_2} = \frac{\omega_2}{\omega_1} = \frac{\mathcal{T}_1}{\mathcal{T}_2}, \tag{1}$$

where ω_i and $\mathcal{T}_i$ are respectively the angular speed and period of gear G_i, related by $\omega_i = 2\pi/\mathcal{T}_i$.

The system has performed a full cycle when both gears have simultaneously come back to their initial configuration, after a period:

$$\mathcal{T}_{12} = n_1\mathcal{T}_1 = n_2\mathcal{T}_2, \tag{2}$$

where n_1 and n_2 are the integer numbers of rotations experienced by each gear. By definition, the minimal value that satisfies this relation is the Least Common Multiple. Therefore:

$$\mathcal{T}_{12} = \mathrm{lcm}(\mathcal{T}_1, \mathcal{T}_2). \tag{3}$$

If we add a new gear G_3, which meshes with one of the existing gears and also influences the drawing pen, all we need to do is compute the new period:

$$\mathcal{T}_{123} = \mathrm{lcm}(\mathcal{T}_{12}, \mathcal{T}_3), \tag{4}$$

and so on for any additional gear.

1.2 Typology of constraints

For each machine, constraints on shape parameters reflect a number of functional and practical features.

Finite pattern. The first requirement is that the drawing can be produced in a reasonable amount of time, and *a fortiori*, a finite one. For each pair of gears, combining Eq. 1 and 2 gives the necessary condition

$$\frac{r_1}{r_2} = \frac{\mathcal{T}_1}{\mathcal{T}_2} = \frac{n_1}{n_2} \in \mathbb{Q}. \tag{5}$$

Table 1: *Main notations used in this document.*

Notation	Meaning
r (resp. $\overline{r}$)	Free (resp. fixed) parameter
A	Geometric point
$\overrightarrow{\mathrm{AB}}$ (resp. $\vec{v}$)	Bound (resp. free) vector
$\|.\|$	Euclidean norm
$\mathfrak{R}$	Reference frame
R_θ	Rotation of angle θ centered at the origin

In other words, if $r_1/r_2 \notin \mathbb{Q}$, the gears will take an infinite amount of turns to come back to their initial configuration.

We incorporate this rationality constraint in our parameterizations by taking gear radii in $\mathbb{N}_{>0}$. This constraint can be extended to non-circular gears, as demonstrated in Sec. 2.2.

Compatible curvatures. Although, in classic mechanisms, non-circular gears often come in pairs with conjugate profiles, interesting trajectories can be obtained when rolling such a gear along a shape of different type. However, all not shapes can be rolled along each other without interference. Let us consider the case of an ellipse $\mathcal{E}_1$ rolling inside another ellipse $\mathcal{E}_2$. We can formulate the curvature compatibility constraint as

$$\kappa_{min}^{\mathcal{E}_1} \geq \kappa_{max}^{\mathcal{E}_2}.$$

This constraint ensures that at the point where the moving ellipse is the 'straightest', or least curved, it can still fit wherever the fixed enclosing ellipse is the most curved. While necessary, this constraint is not sufficient in more general cases, where *ad hoc* conditions should be added to avoid collisions.

Symmetry and congruence reduction. For a single machine, the space of available patterns can be very diverse but also highly redundant. This is typically caused by symmetries in the mechanical layout, or parameter combinations giving patterns that only differ by an affine transformation. Whenever this is possible, we put constraints on the parameters to remove such redundancies.

Valid layout. This type of condition only considers the abstract geometric model. It prevents components belonging to the same layer from overlapping. These are only basic constraints though, as in practice, collision avoidance depends on the specific physical implementation of the machine.

Drawing bounds. The size of the canvas is bounded, and the pen should never leave this drawing area.

Singularity avoidance. This problem has already been described in previous works [Bächer et al. 2015]. Singular configurations typically happen when two links become perfectly aligned, which should be avoided (be it in the simulation or in real life).

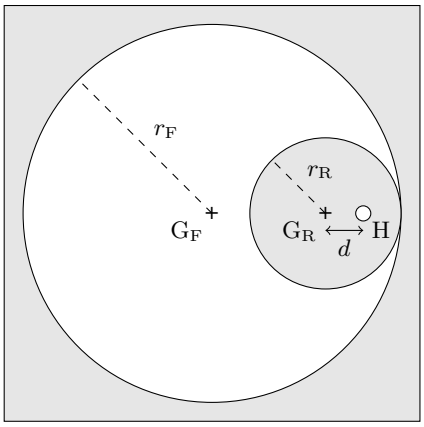

Figure 1: *Dimensions of a basic Spirograph (in the case where the moving gear rolls inside the fixed one).*

Practical dimensions. Lastly, although some parameters could grow indefinitely without being limited by one of the previous constraints, we set some arbitrary bounds to ensure that the machine keeps a reasonable size.

The constraints are not always easy to evaluate. For instance, in the general case, the "drawing bounds" condition would require to produce the pattern in order to estimate whether or not the bounds are satisfied. This poses a chicken-and-egg problem, since we want to compute a pattern only if the constraints are satisfied. As a consequence, every time this situation arose, we determined a sufficient condition that only depends on the shape parameters.

1.3 Notations

See Table 1 for the main notations. To improve the readability of equations, we sometimes make the following simplifications:

- all vectors are expressed in a fixed reference frame $\mathfrak{R}_0$ unless stated otherwise,
- all variable vectors and scalars of kinematic equations are time functions taken defined over $[0, \mathcal{T}]$, where $\mathcal{T}$ is the period defined in Section 1.1.

2 Drawing machines

2.1 Basic Spirograph

The Spirograph is a 1965 drawing toy developed by Denys Fisher. Nowadays, the Spirograph is a complete set composed of various toothed plastic shapes. In our work, however, we focused on the "classic" version: a gear rolling without slipping inside or outside a circular ring.

Design parameters. Three parameters completely describe the figures drawn by a classic Spirograph (factoring out rigid transformations). See Table 2 for symbols and Figure 1 for a geometric representation.

Constraints. The following constraints are grouped under the categories outlined in Section 1.2.

Table 2: *Symbols for the Spirograph model.*

Component	Geometric center
Fixed gear	$\mathrm{G_F}$
Rolling gear	$\mathrm{G_R}$
Pen hole	H

Parameter	Meaning
r_F	Radius of the fixed gear's primitive
r_R	Radius of the rolling gear's primitive
d	Distance between $\mathrm{G_R}$ and H

- Finite pattern:

$$r_\mathrm{F},\ r_\mathrm{R} \in \mathbb{N}_{>0}, \tag{6}$$
$$r_\mathrm{F} < \mathcal{B}_r, \tag{7}$$

  where $\mathcal{B}_r$ is an arbitrary integer constant.

- Valid layout:

$$0 < r_\mathrm{R} < r_\mathrm{F}, \tag{8}$$
$$|d| \leqslant r_\mathrm{R}. \tag{9}$$

- Symmetry and congruence reduction:

$$\gcd(r_\mathrm{F}, r_\mathrm{R}) = 1, \tag{10}$$
$$d > 0. \tag{11}$$

Kinematic equations. The basic Spirograph produces curves called *trochoids* (*hypotrochoids* if the gear rolls inside the ring, and *epitrochoids* if it rolls outside the ring). The parametric equation of a trochoid in Cartesian coordinates is:

$$\vec{\gamma}(t) \coloneqq \overline{r_\mathrm{R}}(\overline{q} \mp 1) \begin{bmatrix}\cos(t)\\ \sin(t)\end{bmatrix} + \overline{d} \begin{bmatrix}\pm\cos\left((\overline{q} \mp 1)\, t\right)\\ -\sin\left((\overline{q} \mp 1)\, t\right)\end{bmatrix} \quad t \in [0, \mathcal{T}], \tag{12}$$

where $\overline{q} = \overline{r_\mathrm{F}}/\overline{r_\mathrm{R}}$, and the upper and lower operators respectively denote the hypo- and epitrochoid cases.

2.2 Elliptic Spirograph

This slight variation of the base Spirograph does not correspond to a particular commercial toy. We developed it as a simple extension that adds one continuous parameter to the previous model. For this reason, we voluntarily constrained the pen hole to lie on the major axis of the elliptic primitive. However, the geometric analysis gets already more involved than in the basic case.

Design parameters. The elliptic Spirograph is described by four parameters defining the layout and dimensions of two components. See Table 3 for symbols and Figure 2 for a geometric representation.

Ellipses are usually described by their semi-minor and semi-major axes a and b. However, the finite-curve constraint is more complex to write in terms of these parameters. For non-circular gears, Eq. 5 can be generalized to

$$\frac{P_1}{P_2} = \frac{\mathcal{T}_1}{\mathcal{T}_2} = \frac{n_1}{n_2} \in \mathbb{Q} \tag{13}$$

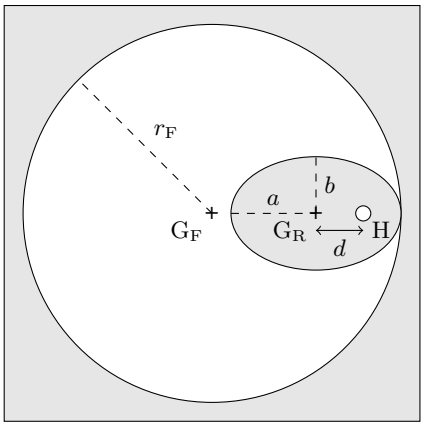

Figure 2: *Dimension of the elliptic Spirograph model.*

where P_i is the perimeter of gear i. For an elliptic profile, it is given by

$$P = 4aE(e), \tag{14}$$

where E is the well-known complete elliptic integral of the second kind:

$$E(k) = \int_0^{\frac{\pi}{2}} \sqrt{1 - k^2 \sin^2\theta} d\theta, \tag{15}$$

and $e = \sqrt{1 - \frac{b^2}{a^2}}$ is the eccentricity of the ellipse.

Thus in practice, we consider the more convenient pair (r_{R}^{eq}, e), where r_{R}^{eq}, the 'equivalent radius', is the radius of a circle with the same perimeter. Therefore r_{R}^{eq} can follow the same condition as the other radii. The link between the two pairs of parameters is given by:

$$2\pi r_{\mathrm{R}}^{eq} = 4aE(e), \tag{16}$$

$$b = a\sqrt{1 - e^2}. \tag{17}$$

Constraints. The following constraints are grouped by the categories outlined in Section 1.2.

- Finite pattern:

$$r_{\mathrm{F}},\ r_{\mathrm{R}}^{eq} \in \mathbb{N}_{>0}, \tag{18}$$

$$r_{\mathrm{F}} < \mathcal{B}_r, \tag{19}$$

  where $\mathcal{B}_r$ is an arbitrary integer constant.

- Compatible curvatures:

$$a < \sqrt{b r_{\mathrm{F}}}. \tag{20}$$

- Valid layout:

$$0 < r_{\mathrm{R}}^{eq} < r_{\mathrm{F}}, \tag{21}$$

$$0 \leqslant e < 1, \tag{22}$$

$$|d| \leqslant a. \tag{23}$$

- Symmetry and congruence reduction:

$$\gcd(r_{\mathrm{F}}, r_{\mathrm{R}}^{eq}) = 1, \tag{24}$$

$$d > 0. \tag{25}$$

Table 3: *Symbols for the elliptic Spirograph model. Parameter pairs marked by * and † can equivalently describe the elliptic primitive.*

Component	Geometric center
Fixed gear	$\mathrm{G_F}$
Rolling gear	$\mathrm{G_R}$
Pen hole	H

Parameter	Meaning
r_{F}	Radius of the fixed gear's primitive
a	Semi-major axis of the rolling gear's primitive*
b	Semi-minor axis of the rolling gear's primitive*
r_{R}^{eq}	Radius of the circle with the same perimeter† as the rolling gear's primitive
e	Eccentricity of the rolling gear's primitive†
d	Distance between $\mathrm{G_R}$ and H

Kinematic equations. As a generalization of trochoids, when a point M is attached to a moving curve Γ_m that rolls without slipping (RWS) along a fixed curve Γ_f, both being in the same plane $\mathcal{P}$, M describes a curve Γ_r in $\mathcal{P}$, called a *roulette curve*. In *The General Theory of Roulettes* [Walker 1937], Walker gives a general method to obtain the parametric equation of roulette curves. We follow the ideas of his demonstration but adapt the equations to our own formulation.

We are looking for an expression of the roulette curve:

$$\vec{\gamma}(t) \coloneqq \overrightarrow{\mathrm{G_F H}}(t) \quad t \in [0, \mathcal{T}]. \tag{26}$$

We first introduce two reference frames:

- $\mathfrak{R}_0$, a frame attached the fixed gear with $\mathrm{G_F}$ as its origin,
- and $\mathfrak{R}_{\mathrm{R}}$, a moving frame attached to the rolling gear with $\mathrm{G_R}$ as its origin.

We consider the primitive curves of each gear Γ_{F} and Γ_{R}, initially touching each other at a contact point C_0 with their tangents aligned. Each curve is described in its own reference frame by a differentiable parametric function, namely $\overrightarrow{\gamma_{\mathrm{F}}}$ and $\overrightarrow{\gamma_{\mathrm{R}}}$. At every t, the contact point C travels on both curves, so that:

$$\overrightarrow{\mathrm{G_F C}}(t) = \overrightarrow{\gamma_{\mathrm{F}}}(t) = \left[\overrightarrow{\gamma_{\mathrm{R}}}(t)\right]_{\mathfrak{R}_0}, \tag{27}$$

where $[.]_{\mathfrak{R}_0}$ denotes the reference frame. More specifically, for any point M attached to $\mathfrak{R}_{\mathrm{R}}$:

$$\left[\overrightarrow{\mathrm{G_F M}}\right]_{\mathfrak{R}_0} = \overrightarrow{\mathrm{G_F G_R}}(t) + R_{\phi_{\mathrm{FR}}(t)}\left(\left[\overrightarrow{\mathrm{G_R M}}\right]_{\mathfrak{R}_{\mathrm{R}}} - \overrightarrow{\mathrm{G_F G_R}}(t)\right), \tag{28}$$

where $\phi_{\mathrm{FR}}(t)$ is the oriented angle between $\mathfrak{R}_0$ and $\mathfrak{R}_{\mathrm{R}}$ at t. Since the tangents to each curve at C_0 must always be aligned, the rotation should compensate for the angular difference between the tangents in their own reference frame. Therefore:

$$\phi_{\mathrm{FR}}(t) = -\left(\phi_{\mathrm{F}}(t) - \phi_{\mathrm{R}}(t)\right) \quad \forall t, \tag{29}$$

where ϕ_{F} and ϕ_{R} are the tangential angles of $\overrightarrow{\gamma_{\mathrm{F}}}$ and $\overrightarrow{\gamma_{\mathrm{R}}}$ respectively.

Applying Eq. (28) to $\overrightarrow{\gamma_{\mathrm{R}}}$ and using the coincidence relation Eq. (27) gives:

$$\overrightarrow{\gamma_{\mathrm{F}}}(t) = \overrightarrow{\mathrm{G_F G_R}}(t) + R_{\phi_{\mathrm{FR}}(t)}\left(\overrightarrow{\gamma_{\mathrm{R}}}(t) - \overrightarrow{\mathrm{G_F G_R}}(t)\right) \quad \forall t. \quad (30)$$

Then, we can evaluate Eq. (28) at point H, substract the above equation to get rid of $\overrightarrow{\mathrm{G_F G_R}}$, and finally use the curve definition Eq. (26) to write:

$$\overrightarrow{\gamma}(t) \coloneqq \overrightarrow{\gamma_{\mathrm{F}}}(t) + R_{\phi_{\mathrm{FR}}(t)}\left(\left[\overrightarrow{\mathrm{G_R H}}\right]_{\mathfrak{R}_{\mathrm{R}}} - \overrightarrow{\gamma_{\mathrm{R}}}(t)\right) \quad \forall t. \quad (31)$$

Eq. (31) allows us to compute the roulette once the specific gear profile parameterizations γ_{F} and γ_{R} are known. It does not, however, tell us how the RWS condition is enforced. Following this constraint, the contact point must travel on both curves at the same speed, meaning that:

$$\left\|\overset{\bullet}{\overrightarrow{\gamma_{\mathrm{F}}}}(t)\right\| = \left\|\overset{\bullet}{\overrightarrow{\gamma_{\mathrm{R}}}}(t)\right\| \quad \forall t. \quad (32)$$

Integrating this equation translates into an equality of arc lengths for all t. Therefore we introduce a common arc length function:

$$\Lambda : \begin{cases} [0, \mathcal{T}] \to [0, \mathcal{L}] \\ t \mapsto \Lambda(t) = \Lambda_{\mathrm{F}}(t) = \Lambda_{\mathrm{R}}(t) \end{cases} \quad (33)$$

where $\mathcal{L}$ is the total distance traveled during the drawing. Using the fundamental theorem of calculus, it is easy to show that the arc length function is continuous and strictly monotone, and therefore bijective. We use the reciprocal function to implement the RWS condition via a change of variables:

$$\overrightarrow{\gamma_*}'(s) \coloneqq \overrightarrow{\gamma_*} \circ \Lambda^{-1}(s) \quad \forall s \in [0, \mathcal{L}], \quad (34)$$

where s is called the *arc length parameter*, and is the same for both curves.

Finally, the roulette curve in Eq. (31) becomes:

$$\overrightarrow{\gamma}'(s) \coloneqq \overrightarrow{\gamma_{\mathrm{F}}}'(s) + R_{\phi_{\mathrm{FR}}(s)}\left(\left[\overrightarrow{\mathrm{G_R H}}\right]_{\mathfrak{R}_{\mathrm{R}}} - \overrightarrow{\gamma_{\mathrm{R}}}'(s)\right) \quad s \in [0, \mathcal{L}]. \quad (35)$$

The above developments are purely theoretical, and could be applied to gears of various primitive shapes, as long as they have compatible curvatures and do not collide during the drawing. Let us now demonstrate the case of the elliptic Spirograph. The basic parameterizations are:

$$\overrightarrow{\gamma_{\mathrm{F}}}(t) \coloneqq \overline{r_{\mathrm{F}}} \begin{bmatrix} \cos(t) \\ \sin(t) \end{bmatrix} \quad t \in [0, \mathcal{T}], \quad (36)$$

and

$$\overrightarrow{\gamma_{\mathrm{R}}}(t) \coloneqq \begin{bmatrix} \overline{a}\cos(t) \\ \overline{b}\sin(t) \end{bmatrix} \quad t \in [0, \mathcal{T}]. \quad (37)$$

Transforming Eqs. (36, 37) into arc length parameterizations necessitates to invert their respective arc length functions. While being easy for $\overrightarrow{\gamma_{\mathrm{F}}}(t)$:

$$\Lambda_{\mathrm{F}}(t) \coloneqq \overline{r_{\mathrm{F}}}\, t \qquad \forall t \in [0, \mathcal{T}],$$
$$\Lambda_{\mathrm{F}}^{-1}(s) \coloneqq s/\overline{r_{\mathrm{F}}} \qquad \forall s \in [0, \mathcal{L}],$$

it is more complicated for $\overrightarrow{\gamma_{\mathrm{R}}}(t)$:

$$\Lambda_{\mathrm{R}}(t) \coloneqq \overline{a}\left(E\left(t + \frac{\pi}{2}, \overline{e}\right) - E(\overline{e})\right) \quad \forall t \in [0, \mathcal{T}], \quad (38)$$

where this time $E(\phi, k)$ denotes the *incomplete* elliptic integral of the second kind, function of an amplitude ϕ and an elliptic modulus k. Inverting E with respect to amplitude is theoretically possible; however, as noted in an article by Ghrist et al. [Ghrist and Lane 2013], while inverses of elliptic integrals of the first kind are well-known in the literature (and called *Jacobi elliptic functions*), very little has been written on their second kind counterparts.

In practice we could compute the inverse of E numerically; however, in this case we opt for a more efficient method, which can be applied to other complicated scenarios. The idea is to keep the original parameterization of the more complex shape, and only invert the arc length function of the simpler one. Here for instance, we keep the ellipse parameterization $\overrightarrow{\gamma_{\mathrm{R}}}$, and use a new circle parameterization

$$\overrightarrow{\gamma_{\mathrm{F}}}' \coloneqq \overrightarrow{\gamma_{\mathrm{F}}} \circ \Lambda_{\mathrm{F}}^{-1} \circ \Lambda_{\mathrm{R}}, \quad (39)$$

which only requires to evaluate E directly. This "trick" allows us to enforce the RWS condition efficiently.

2.3 Cycloid Drawing Machine

The Cycloid Drawing Machine is a relatively recent project by Joe Freedman [2015], with a virtual version by Jim Bumgardner [2015] available online. Despite its name, this machine can produce figures that are far more complex than cycloids, which can be obtained from a simple Spirograph. It allows several configurations, among which we only implemented the simplest one (single gear, fixed fulcrum).

Design parameters. Our configuration of the Cycloid Drawing Machine is described by six parameters, controlling the layout and dimensions of six components. See Table 4 for symbols and Figure 3 for a geometric representation.

Constraints. The following constraints are grouped by the categories outlined in Section 1.2.

- Finite pattern:

$$r_{\mathrm{T}},\ r_{\mathrm{E}} \in \mathbb{N}_{>0}, \quad (40)$$
$$r_{\mathrm{T}},\ r_{\mathrm{E}} < \mathcal{B}_r, \quad (41)$$

  where $\mathcal{B}_r$ is an arbitrary integer constant.

- Valid layout:

$$0 < r_{\mathrm{T}} < d_{\mathrm{TF}}, \quad (42)$$
$$0 < d_{\mathrm{FH}} < d_{\mathrm{FE}} - r_{\mathrm{E}}, \quad (43)$$
$$0 \leqslant r_{\mathrm{S}} < r_{\mathrm{E}}, \quad (44)$$

  with:

$$d_{\mathrm{FE}} \coloneqq \left\|\overrightarrow{\mathrm{FG_E}}\right\| = \left(d_{\mathrm{FH}}^2 + (r_{\mathrm{T}} + r_{\mathrm{E}})^2 - 2d_{\mathrm{FH}}(r_{\mathrm{T}} + r_{\mathrm{E}})\cos\theta_{\mathrm{TE}}\right)^{\frac{1}{2}}$$

- Symmetry and congruence reduction:

$$\gcd(r_{\mathrm{T}}, r_{\mathrm{E}}) = 1, \quad (45)$$
$$0 \leqslant \theta_{\mathrm{TE}} \leqslant \pi. \quad (46)$$

- Drawing bounds:

$$\max_t \left\|\overrightarrow{\mathrm{G_T H}}\right\| < r_{\mathrm{T}}, \quad (47)$$

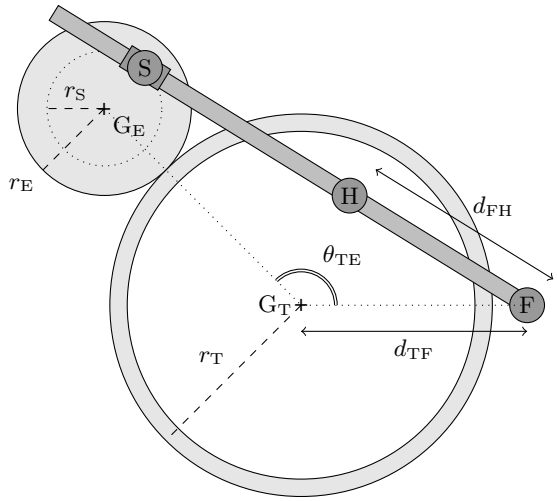

Figure 3: *Dimensions of the Cycloid Drawing Machine model.*

with

$$\operatorname{argmax} \left\| \overrightarrow{\mathrm{G_T H}} \right\| = \begin{bmatrix} d_{\mathrm{TF}} \\ 0 \end{bmatrix} + d_{\mathrm{FH}} \begin{bmatrix} \cos(\theta_{\mathrm{FE}} - \alpha) \\ \sin(\theta_{\mathrm{FE}} - \alpha) \end{bmatrix}, \quad (48)$$

where α is the amplitude of the oscillation:

$$\alpha \coloneqq \arctan\left(\frac{r_{\mathrm{S}}}{d_{\mathrm{FE}}}\right), \quad (49)$$

and θ_{FE} is the polar angle of $\overrightarrow{\mathrm{FG_E}}$:

$$\theta_{\mathrm{FE}} \coloneqq \pi - \arctan\left(\frac{(r_{\mathrm{T}} + r_{\mathrm{E}}) \sin\theta_{\mathrm{TE}}}{d_{\mathrm{TF}} - (r_{\mathrm{T}} + r_{\mathrm{E}}) \cos\theta_{\mathrm{TE}}}\right) \quad (50)$$

- Practical dimensions:

$$d_{\mathrm{TF}} \leqslant \mathcal{B}_d, \quad (51)$$

where $\mathcal{B}_d$ is an arbitrary constant.

Kinematic equations. The Cycloid Drawing Machine and the Hoot-Nanny both use a turntable to increase the complexity of the drawing they produce. The equation of the corresponding curve can be expressed in a general way.

We first consider two frames, sharing the same origin $\mathrm{G_T}$:

- a fixed frame of reference $\mathfrak{R}_0$,
- and a rotating frame of reference $\mathfrak{R}_{\mathrm{T}}$, attached to the turntable.

The polar angle from $\mathfrak{R}_0$ to $\mathfrak{R}_{\mathrm{T}}$ is equal to θ_{T}, the rotation angle of the turntable gear. Since both frames have the same origin, the frame change equation is simpler than for the elliptic Spirograph (*cf.* Eq. 28). For any point M attached to the rotating frame, it comes:

$$[\overrightarrow{\mathrm{G_T M}}]_{\mathfrak{R}_{\mathrm{T}}} = R_{-\theta_{\mathrm{T}}} [\overrightarrow{\mathrm{G_T M}}]_{\mathfrak{R}_0}. \quad (52)$$

We can then define the drawing obtained from turntable-based machines as the curve:

$$\vec{\gamma}(t) \coloneqq [\overrightarrow{\mathrm{G_T H}}(t)]_{\mathfrak{R}_T} \quad t \in [0, \mathcal{T}]. \quad (53)$$

Table 4: *Symbols for the Cycloid Drawing Machine model.*

Component	Geometric center
Turntable gear	$\mathrm{G_T}$
External gear	$\mathrm{G_E}$
Fulcrum (or pivot)	F
Slider	S
Pen-holder	H

Parameter	Meaning
r_{T}	Radius of the turntable gear's primitive
r_{E}	Radius of the external gear's primitive
d_{TF}	Distance between $\mathrm{G_T}$ and F
θ_{TE}	Polar angle of $\overrightarrow{\mathrm{G_T G_E}}$
r_{S}	Distance between $\mathrm{G_E}$ and S
d_{FH}	Distance between F and H

Let us now express $\vec{\gamma}(t)$ as a function of the shape parameters. We have

$$\begin{aligned} \overrightarrow{\mathrm{G_T H}} &= \overrightarrow{\mathrm{G_T F}} + \overrightarrow{\mathrm{FH}} \\ &= \begin{bmatrix} \overline{d_{\mathrm{TF}}} \\ 0 \end{bmatrix} + \overline{d_{\mathrm{FH}}} \frac{\overrightarrow{\mathrm{FS}}}{\left\| \overrightarrow{\mathrm{FS}} \right\|}, \end{aligned}$$

with:

$$\begin{aligned} \overrightarrow{\mathrm{FS}} &= \overrightarrow{\mathrm{FG_T}} + \overrightarrow{\mathrm{G_T G_E}} + \overrightarrow{\mathrm{G_E S}} \\ &= \begin{bmatrix} -\overline{d_{\mathrm{TF}}} \\ 0 \end{bmatrix} + (\overline{r_{\mathrm{T}}} + \overline{r_{\mathrm{E}}}) \begin{bmatrix} \cos\overline{\theta_{\mathrm{TE}}} \\ \sin\overline{\theta_{\mathrm{TE}}} \end{bmatrix} + \overline{r_{\mathrm{S}}} \begin{bmatrix} \cos\theta_{\mathrm{ES}} \\ \sin\theta_{\mathrm{ES}} \end{bmatrix} \end{aligned}$$

where θ_{ES} is the polar angle of $\overrightarrow{\mathrm{G_E S}}$.

All that remains is to express the gear angles as functions of time. Integrating the law of gearing (1) and taking the constant to be 0 yields:

$$\theta_{\mathrm{ES}}(t) = -\frac{\overline{r_{\mathrm{T}}}}{\overline{r_{\mathrm{G}}}} \theta_{\mathrm{T}}(t) \quad \forall t. \quad (54)$$

Finally, if the turntable gear is considered as the driving gear, θ_{T} can be simply taken as:

$$\theta_{\mathrm{T}}(t) \coloneqq t \quad \forall t \in [0, \mathcal{T}]. \quad (55)$$

While a dedicated driving gear can be added for convenience, it does not influence the aspect of the drawing and therefore is not considered in this model.

2.4 Hoot-Nanny

The Hoot-Nanny, also known as Magic Designer, is an older toy from the middle of the 20th century, produced and commercialized at the time by Northern Signal Company, Milwaukee. The "trick" of fixing the sheet of paper onto a turntable to increase the complexity of the drawings may have inspired the design of the Cycloid Drawing Machine described above. An online version by Abel Vincze [2016] called "HTML Spirograph" allows to draw an impressive range of beautiful patterns by varying the color and transparency of the curve.

Table 5: *Symbols for the Hoot-Nanny model.*

Component	Geometric center
Turntable gear	$\mathrm{G_T}$
External gear i	G_i
Pivot joint i	P_i
Arm i	A_i
Pen-holder	H

Parameter	Meaning
r_T	Radius of the turntable gear's primitive
r_{G_i}	Radius of external gear i 's primitive
θ_{12}	Angle $\widehat{\mathrm{G_1 G_T G_2}}$
r_{P_i}	Distance between P_i and G_i
l_i	Length of arm i

Design parameters. Our Hoot-Nanny is described by eight parameters, controlling the layout and dimensions of eight components. See Table 5 for symbols and Figure 4 for a geometric representation.

Constraints. The following constraints are grouped by the categories outlined in Section 1.2.

- Finite pattern:

$$r_\mathrm{T},\ r_{\mathrm{G}_i} \in \mathbb{N}_{>0}, \tag{56}$$
$$r_\mathrm{T},\ r_{\mathrm{G}_i} < \mathcal{B}_r, \tag{57}$$

  where $\mathcal{B}_r$ is an arbitrary integer constant.

- Valid layout:

$$r_{\mathrm{P}_i} < r_{\mathrm{G}_i}, \tag{58}$$
$$r_{\mathrm{G}_1} + r_{\mathrm{G}_2} < \left\|\overrightarrow{\mathrm{G_1 G_2}}\right\|, \tag{59}$$
$$r_{\mathrm{G}_i} + r_{\mathrm{P}_i} < l_i < 2r_\mathrm{T} + r_{\mathrm{G}_i} - r_{\mathrm{P}_i}, \tag{60}$$

  with:

$$\left\|\overrightarrow{\mathrm{G_1 G_2}}\right\| = \left(d_{\mathrm{TG}_1}^2 + d_{\mathrm{TG}_2}^2 - 2d_{\mathrm{TG}_1} d_{\mathrm{TG}_2} \cos\theta_{12}\right)^{\frac{1}{2}} \tag{61}$$

  where $d_{\mathrm{TG}_i} \coloneqq r_\mathrm{T} + r_{\mathrm{G}_i}$.

- Symmetry and congruence reduction:

$$\gcd(r_\mathrm{T}, r_{\mathrm{G}_i}) = 1, \tag{62}$$
$$0 \leqslant \theta_{12} \leqslant \pi. \tag{63}$$

- Drawing bounds:

$$\max_t \left\|\overrightarrow{\mathrm{G_T H}}\right\| < r_\mathrm{T}, \tag{64}$$

  for which a sufficient condition can be found by observing that a feasible trajectory of the pen in the fixed reference frame (which is not the same as the drawing curve) is always inscribed in a quadrilateral whose vertices are reached when the triplets $(\mathrm{G}_1, \mathrm{P}_1, \mathrm{H})$ and $(\mathrm{G}_2 1, \mathrm{P}_2, \mathrm{H})$ become respectively aligned. For these points the distances between the gear centers and the pen are extremal, with values $d_{\mathrm{HG}_i}^{ext} = r_{\mathrm{G}_i} \pm l_i$, which makes indeed four combinations. Therefore, all that we need to determine is the position of the four vertices, and find the distance of the one that is farthest from the turntable center. The position of a vertex is obtained by applying the law of cosines to the triangle $\mathrm{HG_2 G_1}$:

$$\overrightarrow{\mathrm{G_T H}} = \overrightarrow{\mathrm{G_T G_2}} + d_{\mathrm{HG}_2}^{ext} R_\alpha \frac{\overrightarrow{\mathrm{G_2 G_1}}}{\left\|\overrightarrow{\mathrm{G_1 G_2}}\right\|}, \tag{65}$$

  where α is the angle $\widehat{\mathrm{HG_2 G_1}}$, given by:

$$\alpha = \arccos\left(\frac{-(d_{\mathrm{HG}_1}^{ext})^2 + \left\|\overrightarrow{\mathrm{G_1 G_2}}\right\|^2 + (d_{\mathrm{HG}_2}^{ext})^2}{2 d_{\mathrm{HG}_2}^{ext} \left\|\overrightarrow{\mathrm{G_1 G_2}}\right\|}\right). \tag{66}$$

  We can then reformulate the sufficient condition as:

$$\max_{\mathrm{H}\in\mathcal{V}} \left\|\overrightarrow{\mathrm{G_T H}}\right\| < r_\mathrm{T} \tag{67}$$

  where $\mathcal{V}$ denotes the set of vertices.

- Singularity avoidance:

$$\min_t \left\|\overrightarrow{\mathrm{P_1 H}} \times \overrightarrow{\mathrm{P_1 P_2}}\right\| > 0, \tag{68}$$

  for which a sufficient condition is:

$$\left\|\overrightarrow{\mathrm{G_1 G_2}}\right\| + r_{\mathrm{P}_1} + r_{\mathrm{P}_2} < l_1 + l_2, \tag{69}$$

  reflecting the fact that the arms need to be long enough to prevent alignment when the pivots are farthest from each other.

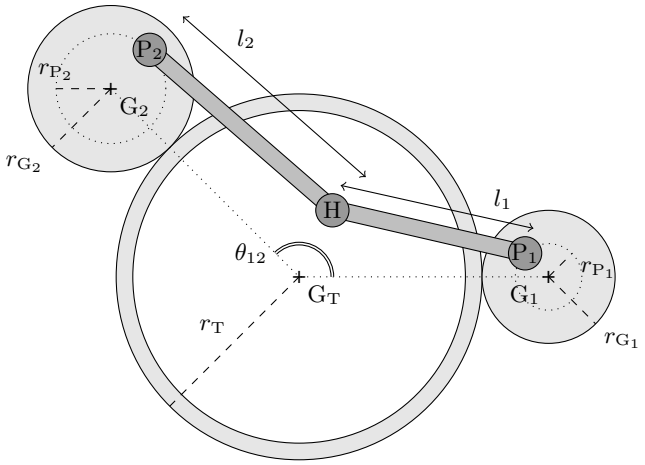

Figure 4: *Dimensions of the Hoot-Nanny model.*

Kinematic equations. As with the Cycloid Drawing Machine, we introduce the rotation angle of each external gear: θ_1 and θ_2. Again, they can be simply related by integrating the law of gearing (1) and taking the constant to be 0:

$$\theta_i(t) = -\frac{\overline{r_\mathrm{T}}}{\overline{r_{\mathrm{G}_i}}} \theta_\mathrm{T}(t) \quad \forall t. \tag{70}$$

Let us now express the curve function (53) via the gears' angles. First, the law of cosines applied to the triangle $\mathrm{HP_2P_1}$ gives

$$\overrightarrow{\mathrm{G_TH}} = \overrightarrow{\mathrm{G_TP_2}} + \overline{l_2} R_\alpha \frac{\overrightarrow{\mathrm{P_2P_1}}}{\left\| \overrightarrow{\mathrm{P_2P_1}} \right\|}, \tag{71}$$

where α is the angle $\widehat{\mathrm{HP_2P_1}}$, given by:

$$\alpha = \arccos \left(\frac{-\overline{l_1}^2 + \left\| \overrightarrow{\mathrm{P_2P_1}} \right\|^2 + \overline{l_2}^2}{2\overline{l_2} \left\| \overrightarrow{\mathrm{P_2P_1}} \right\|} \right). \tag{72}$$

The remaining vectors are given by:

$$\overrightarrow{\mathrm{G_TP_2}} = (\overline{r_{\mathrm{T}}} + \overline{r_{\mathrm{G_2}}}) \begin{bmatrix} \cos \overline{\theta_{12}} \\ \sin \overline{\theta_{12}} \end{bmatrix} + \overline{r_{\mathrm{P_2}}} \begin{bmatrix} \cos \theta_2 \\ \sin \theta_2 \end{bmatrix} \tag{73}$$

and

$$\overrightarrow{\mathrm{P_2P_1}} = (\overline{r_{\mathrm{T}}} + \overline{r_{\mathrm{G_1}}}) + \overline{r_{\mathrm{P_1}}} \begin{bmatrix} \cos \theta_1 \\ \sin \theta_1 \end{bmatrix} - \overrightarrow{\mathrm{G_TP_2}}. \tag{74}$$

References

BÄCHER, M., COROS, S., AND THOMASZEWSKI, B. 2015. Linkedit: Interactive linkage editing using symbolic kinematics. *ACM Trans. Graph. 34*, 4 (July), 99:1–99:8.

BUMGARDNER, J., 2015. CDMS: Built with Processing and Processing.js. http://wheelof.com/sketch. Accessed: 2017-05-02.

FREEDMAN, J., 2015. Cycloid drawing machine. http://leafpdx.bigcartel.com/product/cycloid-drawing-machine. Accessed: 2017-05-02.

GHRIST, M. L., AND LANE, E. E. 2013. Be Careful What You Assign: Constant Speed Parametrizations. *Mathematics Magazine 86*, 1, 3–14.

VINCZE, A., 2016. HTML spirograph. http://htmlspirograph.com. Accessed: 2017-05-02.

WALKER, G. 1937. The General Theory of Roulettes. *National Mathematics Magazine 12*, 1, 21–26.